

Diffusive media characterization with laser speckle

Charles A. Thompson, Kevin J. Webb, and Andrew M. Weiner

The statistical properties of laser speckle with partially coherent light are related to the scattering characteristics of an optically diffuse material. A diffusion equation model is shown to yield a speckle contrast ratio that agrees well with measurements of opaque plastics of varying thicknesses. We show that partially coherent light can be used to determine material parameters for highly scattering media. Measured data for stratified materials with differing scattering properties indicate that this technique may be useful in detecting inhomogeneities. © 1997 Optical Society of America

1. Introduction

Optical imaging within or through scattering media is important in many remote sensing applications. In a heavily scattering medium, where the diffusion equation describes photon propagation, geometric information of embedded objects is not evident in the optical image. This diffusive regime is particularly pertinent to applications such as soft tissue imaging.¹⁻³ In this paper we propose and demonstrate the use of a speckle measurement with partially coherent light to determine either the scattering parameters or the thickness of a highly scattering time-invariant medium. We also perform experiments demonstrating that the speckle contrast ratio can be used to distinguish between different diffusive materials and combinations of these materials. We show results consistent with a model based on the photon diffusion equation.

The coherence properties of laser speckle have been studied previously for applications in imaging correlography, where it is desired to determine the separation of objects within the atmosphere.⁴ In the biomedical field, speckle has been used to diagnose disease in thin, lightly scattering slices (20–40 μm) of skin tissue.⁵ In the heavily scattering regime (such

as in thick samples of tissue), the approach when either the background or the object is in motion has been to use a correlation^{6,7} or a difference^{8,9} in speckle patterns to give a time-resolved image. For static samples, Genack has shown an empirical relation between the intensity autocorrelation and sample thickness when the frequency of a laser line is changed by as much as 30 GHz.¹⁰ The measurement was performed over a domain approximately the size of a speckle spot. The temporal intensity autocorrelation, also measured over a small spot approximately the size of one coherence area, has been related to the solution of the diffusion equation through a path-length distribution by Bellini *et al.*¹¹ The work of Genack and Bellini *et al.* suggests that the coherence properties of light can be used to characterize the optical properties of a highly scattering medium, a concept that is expanded on here.

A measure typically used to describe the degree of coherence of laser speckle is the intensity contrast ratio (σ_I/μ_I), where σ_I is the standard deviation and μ_I is the ensemble average of intensity over the speckle pattern. In a situation where the light is perfectly coherent, the speckle contrast maintains a value of 1, provided there is sufficient scatter for fully developed statistics. With high scatter the real and the imaginary components of the field at each point have a Gaussian probability density with zero mean. If the field magnitude and phase random variables are assumed independent, the intensity probability density function for monochromatic speckle is negative exponential. The top left of Fig. 1 shows a sketch of intensity as a function of position for a speckle pattern with perfectly coherent light. At the top right of Fig. 1 is the corresponding negative exponential intensity probability density for the per-

When this research was done, the authors were with the School of Electrical and Computer Engineering, Purdue University, West Lafayette, Indiana 47907-1285. C. A. Thompson is now with Sensors and Communications Systems, Hughes Aircraft, El Segundo, California 90215.

Received 19 August 1996; revised manuscript received 22 November 1996.

0003-6935/97/163726-09\$10.00/0

© 1997 Optical Society of America

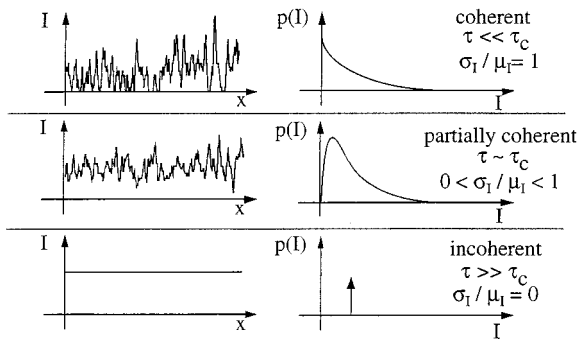


Fig. 1. Comparison between the degrees of optical coherence in a medium with heavy scatter. Left, intensity versus radial position; right, intensity histogram (τ is the standard deviation of photon arrival times; τ_c is the coherence time of the source.)

factly coherent case. If the light is partially coherent, the speckle contrast can have a value somewhere between 0 and 1, depending on the coherence of the source and the degree of scatter experienced by the light,^{12,13} as illustrated in the middle of Fig. 1. Finally, as the medium thickness or the density of scatter increases, the speckle eventually washes out and, in the ideal limit, becomes the mean value of intensity, as depicted at the bottom of Fig. 1.

Speckle contrast measurements have previously been applied for characterization of surface roughness.¹³ In this paper it is demonstrated for the first time to our knowledge that speckle contrast measurements can be used to characterize static, thick scattering media whose behavior follows the photon diffusion equation. To achieve greatest effectiveness, we require that the spread in photon travel times through the medium (τ), which we define as the standard deviation of the arrival time at the output (image) planes (σ_I), be of the same order as the coherence time of the source (τ_c). For $\tau \ll \tau_c$, the contrast approaches 1 (perfectly coherent case), and for $\tau \gg \tau_c$, the contrast tends toward 0 (incoherent case). This means that for our experiments involving highly scattering media with centimeter thicknesses and spreads in photon travel times of hundreds of picoseconds, we can use a simple helium–neon laser with a linewidth of approximately 1 GHz, whereas surface roughness measurements typically employ wideband sources with femtosecond correlation times.

The speckle statistical theory for transmission through diffuse media is developed as an extension of the approach that has been used to represent the case of scattering from a rough surface. The concept of scattering path length is introduced in lieu of surface height variation, where the distribution of path lengths is obtained by employing the Green's function for the diffusion equation. Experimental results for contrast ratio as a function of material thickness then yield the mean optical scattering and absorption parameters for the medium by fitting the path-length density function in an expression derived for σ_I/μ_I .

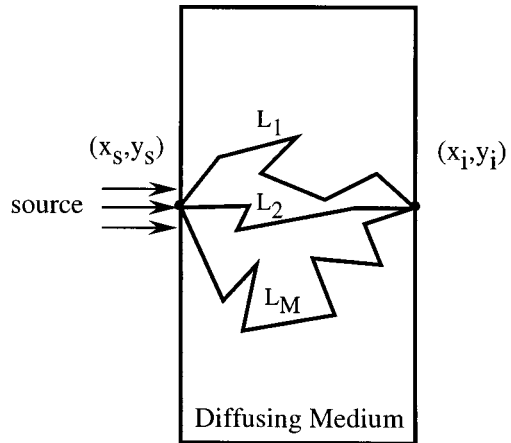


Fig. 2. Diagram of photon diffusion through a random medium. Photons are introduced into the medium by a source located at point (x_s, y_s) . The lines indicate example random paths of photons through the medium. Detection is made at some point (x_i, y_i) on the imaging side of the medium.

2. Theory

When the observation time is large relative to the coherence time of the light, the mean, $\mu_I = \langle I \rangle$, and variance, $\sigma_I^2 = \langle I^2 \rangle - \langle I \rangle^2$, of the intensity of light having finite bandwidth can be expressed as¹³

$$\mu_I(x_i, y_i) = \int_0^\infty S(\lambda) \langle I_n(x_i, y_i, \lambda) \rangle d\lambda, \quad (1)$$

$$\sigma_I^2(x_i, y_i) = \int_0^\infty \int_0^\infty S(\lambda) S(\lambda') \langle U_n(x_i, y_i, \lambda) \times U_n^*(x_i, y_i, \lambda') \rangle^2 d\lambda d\lambda', \quad (2)$$

where $I_n(x_i, y_i, \lambda) = U_n(x_i, y_i, \lambda) U_n^*(x_i, y_i, \lambda)$, $U_n(x_i, y_i, \lambda)$ is the normalized spectral amplitude of the scalar (electric or magnetic) field at image position (x_i, y_i) at wavelength λ , $S(\lambda)$ is the incident power density at wavelength λ from the source, and $\langle \dots \rangle$ is the expected value. In Eq. (1) and arriving at Eq. (2) we assume, by the central limit theorem, that $U_n(x_i, y_i, \lambda)$ is a complex Gaussian process.^{12,13} This implies fully developed statistics, or a sufficiently scattering medium, where the standard deviation in the path length (σ_I) is greater than the maximum wavelength (λ_{\max}). We assume that the real and imaginary components of the field, or the magnitude and phase, are independent or uncorrelated random variables, also as a consequence of significant scatter. With a sufficiently small image area centered at (x_i, y_i) , the mean and variance are invariant over the image spot domain and are represented by the constants μ_I and σ_I^2 , respectively. The field at the detector plane is that at the image point convolved with the deterministic point-spread function for the imaging optics. This point-spread function will scale both μ_I and σ_I by the same constant.

The field at each point at the output of a scattering medium can be represented as a superposition of ran-

dom phasors. Each random phasor can be considered as representing a random photon path through the medium, as depicted in Fig. 2. For a given source illumination,

$$U(x_i, y_i, \lambda) = \sum_{j=1}^M U_j(x_i, y_i, \lambda) \exp[-i2\pi L_j(x_i, y_i, \lambda)], \quad (3)$$

where $U_j(x_i, y_i, \lambda)$ describes the weighting for the random path j , $L_j(x_i, y_i)$ represents the length of the j^{th} random path, and M is a significantly large number of contributing fields. If the photon is not absorbed in the medium, it undergoes only scattering events and exits the medium. Therefore, for a uniform illumination field over a finite aperture, the magnitude of each complex number in the summation of Eq. (3) has the same weighting, or $U_j = U_0$, a constant; the problem can be scaled such that $U_0 = 1$. The sum in Eq. (3) is over those photons that exit the medium, i.e., those that undergo scattering events but no absorption event. If a photon is absorbed in the medium, it is not included in the summation, and it does not contribute to the speckle image. The number of scattered and absorbed photons are dictated by the parameters of the diffuse material. This information is conveyed by the probability density function for the path length. Assume that for partially coherent light the optical parameters of the scattering material can be considered independent of wavelength. The variation of U_j with λ is therefore dictated by the spectrum of the excitation light.

Within the image spot centered at (x_i, y_i) the summation in Eq. (3) can be written as

$$U(\lambda) = U_m(\lambda) \exp(-i2\pi l/\lambda), \quad (4)$$

where l is the path-length random variable and U_m is the field-magnitude random variable. U_m has a Rayleigh density function and the phase $2\pi l/\lambda = \phi(\lambda)$ is uniformly distributed when $\sigma_l \gg \lambda$, which is the case for the diffuse materials of interest.

With an image spot on the output surface of a diffuse material that is small relative to the spatial variation of $\langle I(x_i, y_i, \lambda) \rangle$ and scattering in the medium that is independent of wavelength, set $\langle I_n(x_i, y_i, \lambda) \rangle = I_0$, a constant. With a large image spot, a model describing this spatial variation would be needed; the model proposed herein can be modified for this purpose. For far-field imaging, the Fraunhofer approximation can be used to describe the relationship between the field at the output of the scattering medium and the imaged quantity.

The size of the speckle is related to the imaging optical aperture. The speckle size should be modified to achieve adequate resolution with the detector. For example, the pixel size in an imaging CCD camera should be small relative to the speckle size. We also assume that there is a sufficient amount of speckle within the small image domain for adequate statistics to be formed.

The magnitude, $U_m(\lambda)$, and phase, $\phi(\lambda)$, have been assumed to be independent random variables at each point in the image plane as a consequence of the large

degree of scatter. The speckle properties are dictated by the field autocorrelation at each image point (x_i, y_i) .

Within the small image spot, the mean intensity from Eq. (1) becomes

$$\mu_I = I_0 \int_0^\infty S(\lambda) d\lambda. \quad (5)$$

The normalized field probability density is

$$U_n(\lambda) = I_n^{1/2} \exp[-i\phi(\lambda)], \quad (6)$$

where the normalized intensity random variable $I_n^{1/2}$ is not a function of λ . The expected value of the second moment of $U_m(\lambda)$ becomes

$$\langle U_m^2(\lambda) \rangle = S(\lambda) I_0. \quad (7)$$

The normalized field autocorrelation, $\Gamma_U = \langle U_n(\lambda) U_n^*(\lambda') \rangle$, can then be written as

$$\Gamma_U = \langle I_n \rangle \langle \exp[-i2\pi l(1/\lambda - 1/\lambda')] \rangle. \quad (8)$$

As $\langle I_n \rangle = I_0$,

$$\Gamma_U = I_0 \langle \exp[-i2\pi l(1/\lambda - 1/\lambda')] \rangle. \quad (9)$$

When Eq. (9) is substituted into Eq. (2) and Eq. (5) is used, the speckle contrast (σ_I/μ_I) becomes

$$\begin{aligned} \mu_I/\sigma_I = & \int_0^\infty \left\{ \int_0^\infty \int_0^\infty S(\lambda) S(\lambda') \right. \\ & \left. \times \langle \exp[-i2\pi l(1/\lambda - 1/\lambda')] \rangle^2 d\lambda d\lambda' \right\}^{1/2} / S(\lambda) d\lambda. \end{aligned} \quad (10)$$

The evaluation of the expected value in Eq. (10) requires the probability density function for the path lengths through the medium, $p(l)$. Even though σ_l/λ is large, so that monochromatic light has a uniform phase density, the quantity $l(1/\lambda - 1/\lambda')$ captures the profile of $p(l)$ because σ_l and $(1/\lambda - 1/\lambda')$ are of the same order.

To predict speckle statistics, a relation between the path length of photons emerging from the medium, $l(x_s, y_s; x_i, y_i)$ in Eq. (10), and the physical scattering and absorption within the medium is needed. For the materials considered, the mean-free path is small relative to the thickness, and the attenuation is low. Therefore the time-domain diffusion equation can be used to give a suitable representation for the distribution of travel times (for the light envelope) at a particular image location (x_i, y_i) .^{1,2} The diffusion equation is

$$\begin{aligned} 1/c \partial \Phi(x, y, z, t) / \partial t - D \nabla^2 \Phi(x, y, z, t) \\ + \mu_a \Phi(x, y, z, t) = Q(x, y, z, t), \end{aligned} \quad (11)$$

where c is the speed of light between scattering events, $\Phi(x, y, z, t)$ is the radiative flux (sometimes referred to as photon fluence rate) in watts per square

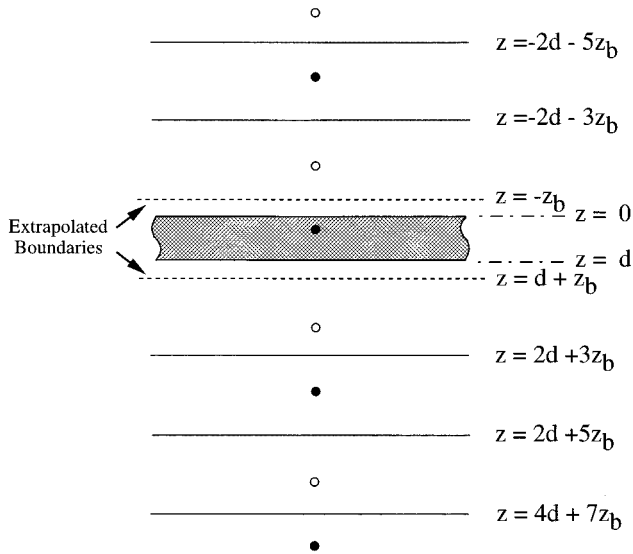


Fig. 3. Schematic of four dipole sources used to produce approximate $\Phi = 0$ boundary conditions on an extrapolated boundary for the diffusion equation model applied to a slab of material. The filled circles represent positive sources, the open circles are negative sources, and the shaded region is the slab of material. The extrapolated boundaries are signified by the dashed lines.

centimeter at position (x, y, z) at time t , $Q(x, y, z, t)$ is the source (watts per cubic centimeter), and D is the diffusion coefficient (centimeters). The diffusion coefficient is given by

$$D = \{3[\mu_a + (1 - g)\mu_s]\}^{-1}, \quad (12)$$

where μ_a is the linear absorption coefficient (per centimeter), μ_s is the linear scattering coefficient (per centimeter), and g is the mean cosine of the scattering angle. The mean-free path between scattering events is $z_0 = 3D$ (centimeters). The homogeneous Green's function for Eq. (11), with $Q(x, y, z, t) = \delta(0, 0, 0)$, is

$$\Phi(x, y, z, t) = \frac{c}{(4\pi Dct)^{3/2}} \times \exp(-\mu_a ct) \exp\left(-\frac{x^2 + y^2 + z^2}{4Dct}\right). \quad (13)$$

Note that the correct units for Φ result when the weighting for the point source in joules is factored into Eq. (13).

For a slab geometry of thickness d , a partially reflecting boundary condition can be obtained by setting $\Phi = 0$ on an extrapolated boundary.¹⁴ The $\Phi = 0$ condition on the extrapolated boundary $z_b = 2AD$ from the input and output faces can be achieved by introducing dipole image sources,¹ as shown in Fig. 3. A dipole is defined as two point sources separated by $2z_0$ and driven 180° out of phase. The unitless parameter A is defined as

$$A = (1 + r_d)/(1 - r_d), \quad (14)$$

where r_d is the reflection coefficient, defined as

$$r_d = -1.440n^{-2} + 0.710n^{-1} + 0.668 + 0.0636n. \quad (15)$$

Here n is the normalized refractive index of the slab, $n = n_1/n_2$, where n_1 is within the medium and n_2 is the index of the background (assumed air for these experiments). The form for Eq. (15) was determined by Egan,¹⁵ using a curve fitted to data presented by Orchard,¹⁶ which related the diffuse reflectance of a slab against the index of the composed material. We have verified the form of Eq. (15) by performing our own independent curve fit to the Orchard data. The slab is assumed to have infinite width. To employ Green's functions for a homogeneous domain, we introduce image sources as dipoles located at $z_d = 2qd + (4q - 1)z_b \pm z_0$, where $z_0 = 3D$ (one transport mean-free path), d is the slab thickness, and q is an integer. In the example presented here, the infinite set of image sources is truncated to four dipoles, corresponding to $q = \{-1, 0, 1, 2\}$. The influence of μ_a damps the signal from sources of larger q value at the physical slab boundaries, resulting in a negligible contribution from these sources. The photon fluence rate for the slab medium, Φ_s , represented as due to four dipoles in an infinite homogeneous domain, is

$$\Phi_s(x, y, z, t) = \sum_{q=-1}^2 \Phi\{x, y, z - [2qd + (4q - 1)z_b + z_0], t\} - \Phi\{x, y, z - [4qd + (2q - 1)z_b - z_0], t\}, \quad (16)$$

where $\Phi(x, y, z - z_d, t)$ represents a dipole at $z = z_d$. The measured transmitted light corresponds to the output photon current density, $T(x, y, d, t)$ in watts per square centimeter, which can be expressed with Fick's law as

$$T(x, y, d, t) = \hat{\mathbf{z}} \cdot [-D\nabla\Phi_s(x, y, z, t)]|_{z=d}, \quad (17)$$

where $\hat{\mathbf{z}}$ is the unit vector in the positive direction and the light is incident upon the slab from the negative z direction.

The intensity distribution as a function of time at position (x, y) on the output plane can be determined by normalizing Eq. (17) over time:

$$f(t) = \frac{T(x, y, d, t)}{\int_0^\infty T(x, y, d, t) dt}. \quad (18)$$

The function $f(t)$ in Eq. (18) gives a density for the number of photons exiting the medium as a function of time. As a measure of the probability density function for l , we set

$$p(l) = f(t)|_{t=l/c}, \quad (19)$$

with $c = c_0/n$, where n is the refractive index of the background medium in which the scattering centers are suspended and c_0 is the speed of light in vacuum. Note that $f(t)$ is a function of μ_a and μ_s , so it provides the distribution of the output optical intensity, ac-

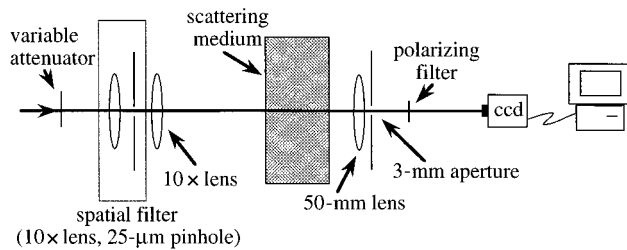


Fig. 4. Diagram of the speckle imaging system. The system images a 1-mm-square spot from the back side of the scattering medium onto the CCD array.

counting for those photons that have undergone absorption events. In the case of complex geometries, this probability density of photon travel times can be solved for numerically. The characteristic function in Eq. (10) can now be expressed as

$$\left\langle \exp \left[-i2\pi l \left(\frac{1}{\lambda} - \frac{1}{\lambda'} \right) \right] \right\rangle = \int_0^\infty p(l) \times \exp \left[-i2\pi l \left(\frac{1}{\lambda} - \frac{1}{\lambda'} \right) \right] dl, \quad (20)$$

clearly showing dependence on the path length in the medium, l , and the coherence length of the light, $l_c \sim \lambda^2/(\Delta\lambda)$, where $\Delta\lambda$ is the bandwidth. With a change of variable, Eq. (20) can be considered the single-sided Fourier transform of $p(l)$.

3. Experiment

Experiments were performed to verify contrast dependence on diffuse media by placing sheets of various plastics at the image plane of an Optronics TEC-470 CCD camera setup, as shown in Fig. 4. A spatially filtered and collimated 30-mW, cw He-Ne laser running at 632.8 nm was used as the illumination source. Experiments were performed with minimal ambient light. A polarizing filter was placed before the CCD camera to increase the contrast of the detected signal. The speckle size was determined by the 3-mm aperture in the output screen, the size of which gave an adequate speckle size for both the resolution and the generation of statistics. The CCD camera (with 640×480 pixels) was set to integrate for 30 s, and the signal was transferred to a PC with an 8-bit frame grabber card for statistical data analysis. The image spot size was approximately 1 mm square. All experiments were performed with the CCD aligned with the excitation laser beam, so that $x = y = 0$ in Eq. (17).

Figure 5 shows example snapshots of speckle patterns measured with this system for two different plastic thicknesses. From the two snapshots, it becomes apparent that the thicker medium shows evidence of the speckle pattern becoming less distinct, or washed out.

The polarizer was used in the system to remove orthogonally (to the incident-laser signal) polarized

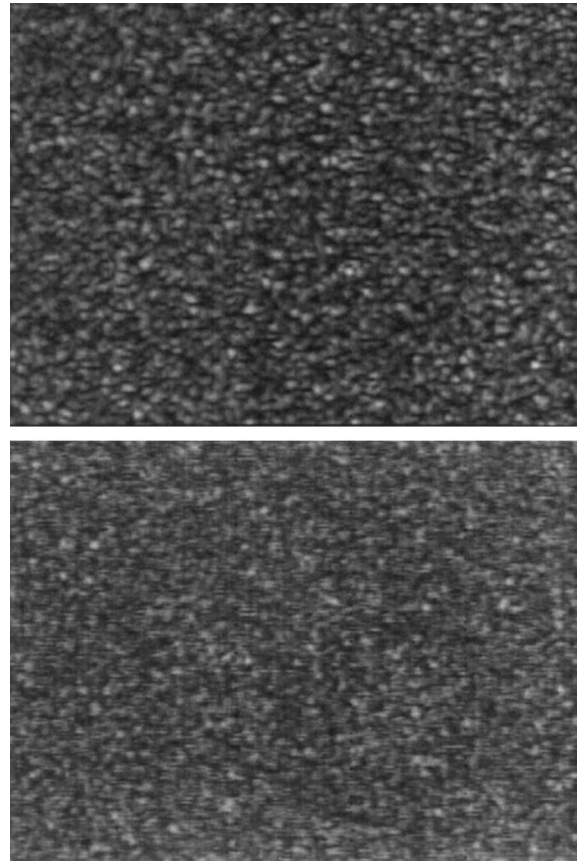


Fig. 5. Snapshot showing typical speckle patterns. Top, Acrylite, 0.6 cm thick; bottom, Acrylite, 3.6 cm thick. Note that the intensity is more uniform (σ_I is smaller) for the thicker sample.

components. The medium had sufficient scatter and was thick enough that the polarization of the light exiting the medium was assumed random. This was experimentally verified by recording speckle patterns with the polarizer set parallel and perpendicular to the incident light. The results for the material thicknesses used show equivalent speckle statistics for both polarizations; i.e., in the diffuse regime where $d \gg z_0$, we expect complete depolarization. The experiment would be equally valid if the polarizer were removed and the resulting speckle pattern considered the incoherent superposition of the parallel and perpendicular polarization components.

The first set of measurements was performed to establish a relationship between material thickness and speckle contrast. Different thicknesses of a highly diffuse white acrylic, Acrylite 0152 by Cyro Industries, were characterized. The various thicknesses were achieved by clamping together several 18 cm \times 18 cm sheets of 0.6-cm-thick material. All sheets came from the same stock to ensure uniform scattering parameters. Figure 6 shows a plot of the measured speckle contrast versus acrylic thickness for several independent (dismantle and reassembly) measurements. An approximate theoretical fit to the speckle contrast data from a least-squares fit to Eq. (10) and Eq. (19) is shown as the dashed curve in

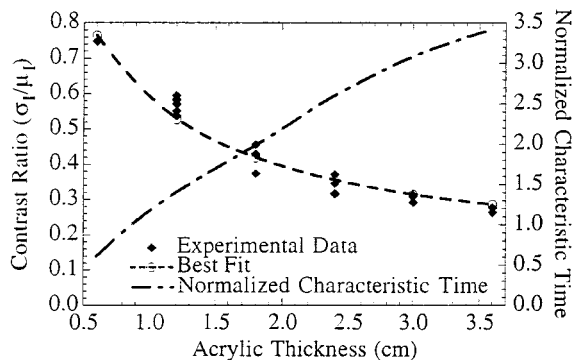


Fig. 6. Speckle contrast ratio (σ_I/μ_I) for various thicknesses of white acrylic. The diamonds represent raw experimental data. The dashed curve is a best fit to the experimental data. This curve gives $\mu_a = 0.005 \text{ cm}^{-1}$ and $\mu_s' = 41.0 \text{ cm}^{-1}$. The normalized characteristic time, τ/τ_c , is plotted on the right axis, where τ is the spread in photon travel times (calculated using $\mu_a = 0.005 \text{ cm}^{-1}$ and $\mu_s' = 41.0 \text{ cm}^{-1}$) and $\tau_c \approx 737 \text{ ps}$ is the laser coherence time.

Fig. 6. The refractive index used in Eq. (15) for the acrylic was $n = 1.49$, determined by measuring the Brewster's angle. Our best fit was obtained with $\mu_s' = \mu_s(1 - g) = 41 \text{ cm}^{-1}$ and $\mu_a = 0.005 \text{ cm}^{-1}$, resulting in $z_0 \approx 0.25 \text{ mm}$. A generous estimation for the bounds for these measurements was determined by calculation of the extremes that fully encompass the experimental data presented in Fig. 6. These bounds are approximately $35 \text{ cm}^{-1} < \mu_s' < 45 \text{ cm}^{-1}$ and $0.002 \text{ cm}^{-1} < \mu_a < 0.007 \text{ cm}^{-1}$. Figure 6 also shows a plot (dotted-dashed curve) of the standard deviation in photon arrival times ($\tau = \sigma_t$) normalized to the coherence time of the laser (τ_c). This normalized characteristic time is calculated with the diffusion equation model and our best fit for μ_a and μ_s' , as given above, used to compute τ . The FWHM lasing bandwidth of the laser was measured to be approximately $\Delta\nu = 900 \text{ MHz}$, with a mode spacing of 161 MHz . This results in a free-space coherence length of approximately 22.1 cm (14.85 cm in the plastic), calculated with $\tau_c = 0.664/\Delta\nu$, which assumes a Gaussian spectral profile.¹⁷ In the simulation the power spectrum was modeled as a pure Gaussian function. For our range of thicknesses τ/τ_c varies from approximately 0.5 to 3.5 , consistent with our premise that the speckle contrast is most sensitive to variations in scattering when τ/τ_c is of the order of unity.

Example measured histograms of speckle intensity for each thickness are shown in Fig. 7. As can be seen in the histograms, σ_I decreases with increasing plastic thickness. Note that the mean intensity values were maintained nearly the same for all thicknesses. The absolute pixel intensity scale is not significant, as it is a result of the linearization process (see Section 4). Figure 8 shows example path-length probability density functions determined using Eq. (19) with Eqs. (16)–(18) for different thicknesses of the acrylic. As expected, the thicker the medium,

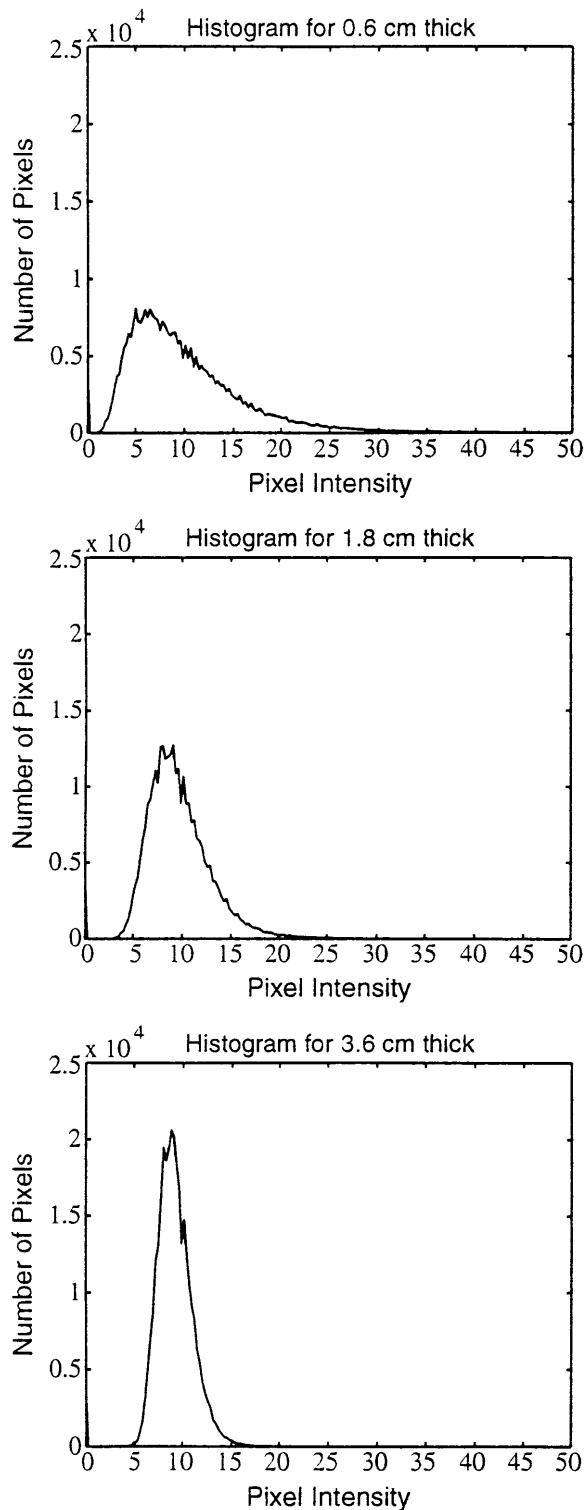


Fig. 7. Example intensity histograms for several Acrylite slab thicknesses. Note that σ_I reduces as the material thickness increases.

the larger the spread in photon arrival times or path length (τ or σ_I).

To confirm our approach, we compared our results with values for the scattering parameters for this material derived by another method, in which the

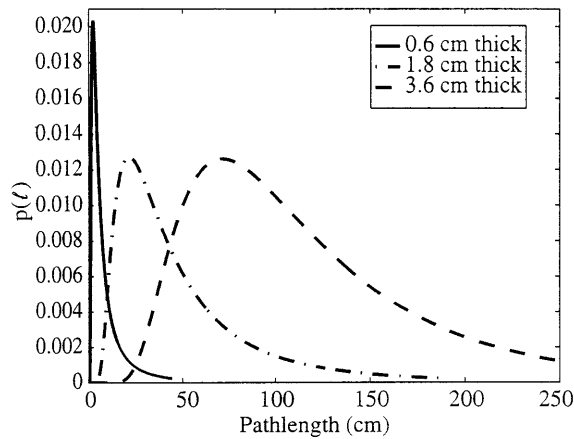
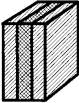
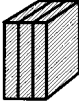
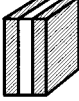


Fig. 8. Probability density functions for photon path lengths, $p(l)$, through three thicknesses of the Acrylite material (0.6, 1.8, and 3.6 cm), calculated using $\mu_s' = 41 \text{ cm}^{-1}$ and $\mu_a = 0.005 \text{ cm}^{-1}$. As the material increases in thickness, σ_l increases.

intensity decay across the surface was measured and fitted to the diffusion equation Green's function solution for a homogeneous domain.¹⁸ These measurements yielded $\mu_s' \approx 15 \text{ cm}^{-1}$ and $\mu_a \approx 0.05 \text{ cm}^{-1}$, with an uncertainty that was estimated to be upwards of 50%. We believe the differences between these scattering parameters and those derived by the speckle method are within the experimental uncertainties of the two techniques. Some of the discrepancy may be attributed to the treatment of the boundary conditions in the diffusion equation modeling. As discussed above, our analysis used a series of four dipole image sources to approximate extrapolated $\Phi = 0$ boundary conditions, rather than a less accurate homogeneous domain model.¹⁸ In addition, the Acrylite-air and air-Acrylite interfaces between the various sheets cause the measured parameters for the stratified sample to differ to some degree from those for a single material layer of the same total thickness. The interfaces introduce reflections that likely increase the path length of obliquely-incident photons, thereby resulting in a larger μ_s' than would be achieved with a single layer.

An additional experiment was performed to illustrate sensitivity to a material hidden within another diffuse material. Two 0.6-cm-thick white acrylic sheets were placed in the center of two pieces of a light white plastic, Plexiglas 2447 by AtoHaaf, each 1.2 cm thick. The scattering parameters of the white Plexiglas were measured to be¹⁸ $\mu_a = 0.02 \text{ cm}^{-1}$ and $\mu_s' = 7.5 \text{ cm}^{-1}$, signifying that the white Plexiglas is less scattering than the white acrylic. The result resembles a plastic sandwich, as shown in column one of Table 1. Speckle contrast is compared with data taken when the center acrylic material is replaced by the white Plexiglas, also 1.2 cm thick (thus making a homogeneous sample) and a clear acrylic (no scattering medium in the center) in Table 1. As expected, the maximum speckle contrast was achieved when the light experienced the least amount of scatter (clear

Table 1. Measured Speckle Contrast Ratio for Plexiglas Containing Various Slabs of 1.2-cm-thick Center Material^a

Center Material	Speckle Contrast ^b (σ/μ)	Characteristic Path Length through Center Material ^c (cm)
 White acrylic	0.3108	8.78
 Homogeneous	0.3503	2.17
 Clear	0.4315	0.00

^aThe contrast ratios are an average of four measurements.

^bAverage of all measurements; the standard deviation of measurements is <0.004 .

^cCalculated by performing a standard deviation of the photon probability density, $p(l)$.

acrylic in the center) and decreased with increasing scatter in the center material.

4. Discussion

Transmission measurements were performed on plastics of differing thickness and composition by the clamping together of a number of sheets. Reflections occur at these interfaces, resulting in a slightly different contrast ratio from that which would be obtained from a single piece of material. There are two competing effects. Fresnel reflections for obliquely incident photons on the plastic-air interface cause these photons to travel farther before they reach the image spot than they would in a single sheet of the same total thickness. This causes the contrast ratio to be lower for the stratified material. However, the Fresnel-reflected photons may be absorbed, or they may escape from a different surface region than they would have in the single-layer case. In this latter case the photons that are more normally incident on the interfaces (those that have on average undergone less scatter) dominate at the image spot. This increases the measured contrast ratio at the image spot. As the μ_a is low for the plastics used, the former effect should dominate, serving to reduce the contrast ratio for the stratified material and hence increase the extracted μ_s' over that for a single slab. An index-matching gel was tried, but flow over the measurement time window washed out the speckle. Ideally, plastics of the appropriate thickness should be used.

The diffusion equation has been used to determine a relationship for the probability density function for photon travel distances through the medium. The diffusion equation, as an approximation of the Bolt-

zmann transport equation, treats the photons as particles. Therefore coherent wave interactions at the optical wavelength cannot be treated directly. However, we assume that the diffusion equation time envelope solution at a point in space, the image point, describes the light passing through the material. The thickness of the material should be greater than ~ 3 mean-free paths ($3z_0$) for the diffusion equation to hold. The fields at the output of the material can be considered as a superposition of a ballistic component and a scattered component. The material thickness is considered large enough (i.e., there are a sufficient number of scattering centers) that the ballistic field can be ignored. The diffusion equation is used to model the heavily scattered field. Views of the speckle patterns for the experiments performed qualitatively support this contention, and the performance of the model presented here in predicting the speckle statistics offers quantitative support. The diffusion equation is used to describe the statistical nature of the imaged intensity; it clearly does not model the actual field structure for a source having a moderately high coherence. As the source coherence decreases, the diffusion equation has been shown to be a good model for the space and time dependence of the light transmitted through a highly scattering medium.²

Consider the use of speckle statistics to characterize a static highly scattering medium, as presented here, in contrast to other optical diffusion imaging approaches that have been explored.^{1,2} The term "diffusion" relates to the high degree of scatter in the medium and hence the applicability of a diffusion equation model to describe the spatial and temporal light envelope for light of low coherence or with local spatial averaging such that the coherent field variation (or speckle) is not detected. The same diffusion equation model is used here to relate the material properties to the measured speckle contrast ratio. The approach that has been used previously in diffusion imaging is to cw modulate a source (say, a light-emitting diode) and make a coherent (magnitude and phase) detection at the modulation frequency.^{1,2} Scanning the source and detector with a single modulation frequency can yield imaging data. For a homogeneous material the variation of the magnitude and phase of the detected signal as a function of detector position, with a fixed source, can be used to determine μ_a and μ_s for the material by means of optimization techniques. The speckle measurements used a partially coherent cw source and provided only magnitude data in the form of σ_I/μ_I at a small image spot on the output face of the material. Using the speckle technique presented here, one can obtain the material parameters by scanning the image spot over the output face of the material with a fixed source location, thereby obtaining the contrast ratio as a function of scan position, or by fixing the image spot and varying the material thickness (as was done to produce the theoretical curve to fit the measured σ_I/μ_I in Fig. 6). To prevent contrast reduction with a dynamic medium, time-gated measurements of speckle could be made and the

coherence of the light could be controlled by modification of the temporal characteristic. It is interesting to note that contrast in the previous photon diffusion imaging techniques^{1,2} depends on the variance of photon travel times relative to the rf modulation frequency, whereas in the current speckle technique contrast depends on the variance in photon travel times relative to the laser coherence time.

The CCD camera used in these experiments exhibited a nonlinear response to intensity, meaning that the relationship between the pixel readings and the optical intensity was nonlinear. To compensate for this nonlinearity, a measured calibration curve of pixel reading as a function of optical intensity was obtained using a series of neutral-density filters. This calibration curve was mapped mathematically to a straight line. Each pixel reading in the measured response therefore had a corresponding linearized intensity; the nonlinear response for the camera was applied to each pixel response. This linearized intensity value for each pixel was used to perform the statistics. With the He-Ne laser and the image spot size used, the CCD required a 30-s integration time. The integration time could be reduced if the laser power were increased or if a more sensitive camera were used. Vibrations cause a washing out of the speckle, i.e., a reduction in the contrast ratio. The optical components were securely mounted on an optical bench to minimize vibrational effects on the measured optical statistics.

The speckle statistics were determined by use of the complete CCD image, which, because of the imaging optics, represents an image spot size at the output surface of the plastic of ~ 1 mm square. The diffusion equation solution for output photon current is slowly varying relative to the image spot size; assumptions of a uniform mean over the image spot at the output of the plastics is accurate for the thick, highly scattering materials used. As an image is formed, it is assumed that the speckle statistics are stationary, or independent of position over the CCD. The point-spread function for the imaging system, convolved with the image field at the output of the diffuse material, gives the true field being imaged. The statistics of the speckle (the correlation of the field) are in general nonstationary, as would be the case for far-field imaging.

The size of the speckle is dictated by the output beam size or limiting aperture. The speckle contrast is determined by the coherence of the light and the scattering properties of the material. Consider light of fixed coherence, as in the experiments presented here. As the limiting aperture in the output imaging system of Fig. 4 is reduced, the speckle size increases. One can equivalently view this as reducing a limiting aperture or reducing the angular spread of photons exiting the scattering medium that are imaged. With a fixed limiting aperture size, increased scatter reduces the contrast ratio. The contrast ratio also reduces with increasing (large) beam size incident on the diffuse plastic.

With sufficiently small material thickness (d) or

scattering coefficient (μ_s'), the diffusion equation model ceases to be valid, necessitating an alternate physical representation. This regime is frequently considered to be $d < 3z_0$. It may also be necessary to consider the correlation between the real and the imaginary field statistics: these fields were considered independent and Gaussian in the model presented here. The speckle data would also be expected to be polarization sensitive, and, in fact, co-polarized and cross-polarized measurements should provide useful characterization data.

In constructing the model for the mean and variance of the speckle intensity at an image point, the first and second moment of the first-order statistics were used, where first order refers to moments evaluated at a single point in space. This was justified because of the slowly varying nature of the first moment or mean over the output surface of the diffuse material. The field correlation, as a function of position and wavelength, is determined by the laser coherence and the path-length density function $p(l)$. By measuring the intensity probability density function as a function of thickness (or position), we generate first-order statistics for the intensity as a function of position. It is the spatial dependence of these first-order statistics that is used to evaluate μ_a and μ_s' for a material through $p(l)$. One could consider using the measured statistics as a function of position with models other than path length derived from the diffusion equation.

5. Conclusion

We have shown that measurements of the speckle contrast as a function of material thickness can be related to a diffusion equation model. Our work suggests that when the laser coherence time is of the order of the spread in photon travel time, speckle contrast can be used to determine the scattering parameters of a material of known thickness or the thickness of a medium with known scattering parameters. Our data also demonstrate that speckle contrast measurements can yield information about the interior structure of scattering samples, potentially leading to a new method of imaging within scattering media.

The authors acknowledge J. Mourant, T. Fuselier, and I. Bigio of Los Alamos National Laboratory for providing their data on the scattering parameters of these plastics and J. P. Robinson of Purdue University Veterinary Sciences for his equipment loan.

References

1. M. S. Patterson, B. Chance, and B. Wilson, "Time-resolved reflectance and transmittance for the noninvasive measurement of tissue optical properties," *Appl. Opt.* **28**, 2331–2336 (1989).
2. J. S. Reynolds, S. Yeung, A. Prasadka, and K. Webb, "Optical diffusion imaging: a comparative numerical and experimental study," *Appl. Opt.* **35**, 3671–3679 (1996).
3. K. Yoo and R. Alfano, "Time-resolved coherent and incoherent components of forward light scattering in random media," *Opt. Lett.* **15**, 320–322 (1990).
4. D. G. Voelz, P. S. Idell, and K. A. Bush, "Illumination coherence effects in laser-speckle imaging," in *Laser Radar VI*, R. J. Bercher, ed., *Proc. SPIE* **1416**, 260–265 (1991).
5. D. A. Zimnyakov, V. V. Tuchin, and S. R. Utts, "A study of statistical properties of partially developed speckle fields as applied to the diagnostics of structural changes in human skin," *Opt. Spectrosc.* **76**, 838–844 (1994).
6. R. Berkovits and S. Feng, "Theory of speckle-pattern tomography in multiple-scattering media," *Phys. Rev. Lett.* **65**, 3120–3123 (1990).
7. D. A. Boas, L. E. Campbell, and A. G. Yodh, "Scattering and imaging with diffusing temporal field correlations," *Phys. Rev. Lett.* **75**, 1855–1858 (1995).
8. P. Naulleau, D. Dilworth, E. Leith, and J. Lopez, "Detection of moving objects embedded within scattering media by use of speckle methods," *Opt. Lett.* **20**, 498–500 (1995).
9. J. D. Briers, "Speckle fluctuations and biomedical optics: implications and applications," *Opt. Eng.* **32**, 277–283 (1993).
10. A. Z. Genack, "Optical transmission in disordered media," *Phys. Rev. Lett.* **58**, 2043–2046 (1987).
11. T. Bellini, M. A. Glaser, N. A. Clark, and V. Degiorgio, "Effects of finite laser coherence in quasi-elastic multiple scattering," *Phys. Rev. A* **44**, 5215–5223 (1991).
12. J. W. Goodman, "Statistical properties of laser speckle patterns," in *Laser Speckle and Related Phenomena*, Vol. 9 of Topics in Applied Physics, J. C. Dainty, ed. (Springer-Verlag, Berlin, 1984).
13. G. Parry, "Some effects of temporal coherence on the first-order statistics of speckle," *Opt. Acta* **21**, 763–772 (1974).
14. T. J. Farrell, M. S. Patterson, and B. Wilson, "A diffusion theory model of spatially resolved, steady-state diffuse reflectance for the noninvasive determination of tissue optical properties *in vivo*," *Med. Phys.* **19**, 879–888 (1992).
15. W. G. Egan and T. W. Hilgeman, *Optical Properties of Inhomogeneous Materials* (Academic, New York, 1979).
16. S. E. Orchard, "Reflection and transmission of light by diffusing suspensions," *J. Opt. Soc. Am.* **59**, 1584–1597 (1969).
17. J. W. Goodman, *Statistical Optics* (Wiley, New York, 1985).
18. J. R. Mourant, J. P. Freyer, and T. M. Johnson, "Measurements of scattering and absorption in mammalian cell suspensions," in *Advances in Laser Light Spectroscopy to Diagnose Cancer and Other Diseases III: Optical Biopsy*, R. Alfano, ed., *Proc. SPIE* **2679**, 79–91 (1996).